Journal of ELECTRONIC MATERIALS, Vol. 31, No. 5, 2002

Regular Issue Paper

535-544

Electronic Applications of Flexible Graphite

XIANGCHENG LUO, RANDY CHUGH, BRIAN C. BILLER, YIE MENG HOI, and D.D.L. CHUNG

Composite Materials Research Laboratory, University at Buffalo, The State University of New York, Buffalo, NY 14260-4400

Flexible graphite is effective for electronic applications, specifically electromagnetic interference (EMI) gasketing, resistive heating, thermoelectric-energy generation, and heat dissipation. It is comparable to or better than conductive-filled silicone materials for EMI gasketing. The shielding effectiveness reaches 125 dB. Flexible graphite as a heating element provides temperatures up to 980°C, response half-time down to 4 sec, and heat output at 60 sec up to 5600 J. The through-thickness, absolute thermoelectric power of flexible graphite is -2.6 μV/°C. Flexible graphite is effective as a thermal-interface material if the thickness is low (0.13 mm), the density is low (1.1 g/cm^3), and the contact pressure is high (11.1 MPa). These applications make use of the flexibility and compliance of flexible graphite, in addition to its electronic and thermal behavior. Compliance is particularly important for the use of flexible graphite as interface materials, whether the interface is electromagnetic, thermoelectric, or thermal.

Key words: Flexible graphite, electronic, EMI, thermoelectric heating, heat dissipation

INTRODUCTION

Flexible graphite is a flexible sheet made by compressing a collection of exfoliated graphite flakes (called worms) without a binder.[1] During exfoliation, an intercalated-graphite flake (graphite compound with foreign species, called the intercalate, between some of the graphite layers) expands typically by over 100 times along the c axis. Compression of the resulting worms (like accordions) causes the worms to be mechanically interlocked to one another so that a sheet is formed without a binder.

Due to the exfoliation, flexible graphite has a relatively large, specific surface area (e.g., 15 m^2/g^2). As a result, flexible graphite is used as an adsorption substrate.[3,4] Due to the absence of a binder, flexible graphite is essentially entirely graphite, other than the ash and the residual amount of decomposed intercalate (such as sulfur in the case of sulfuric acid being the intercalate). As a result, flexible graphite is chemically and thermally resistant and low in coefficient of thermal expansion (CTE). Due to its microstructure involving graphite layers that are preferentially parallel to the surface of the sheet, flexible graphite is high in electrical and thermal conductivities in the plane of the sheet.[5,6] Due to the graphite layers being somewhat connected perpendicular to the sheet (i.e., the honeycomb microstructure of exfoliated graphite), flexible graphite is electrically and thermally conductive in the direction perpendicular to the sheet (although not as conductive as the plane of the sheet).[5,6] These in-plane and out-of-plane microstructures result in resilience and impermeability to fluids perpendicular to the sheet. The combination of resilience, impermeability, and chemical and thermal resistance makes flexible graphite attractive for use as a gasket material for high-temperature or chemically harsh environments.

Gasketing (i.e., packaging and sealing)[7–11] is by far the main application of flexible graphite, which can replace asbestos. Other than gasketing, a number of applications have emerged recently, including adsorption,[3,4] electromagnetic interference (EMI) shielding,[2] vibration damping,[12] electrochemical applications,[13] and stress sensing.[14]

This paper is focused on the electronic applications of flexible graphite, namely, EMI gasketing, re-

(Received November 11, 2001; accepted January 23, 2002)

sistive heating, thermoelectric-energy conversion, and heat dissipation.

ELECTROMAGNETIC INTERFERENCE GASKETING

The EMI shielding is increasingly needed due to the increasing abundance and sensitivity of electronics, particularly radio-frequency devices, which tend to interfere with digital devices. A shielding material needs to be an electrical conductor, although the electrical conductivity does not have to be very high. Due to the skin effect (i.e., the phenomenon that high-frequency electromagnetic radiation only interacts with the surface region of a conductor), a high-surface area of the conductor is desirable. As the electrical conductivity (especially that in the plane of the sheet) and specific surface area are both quite high in flexible graphite, the effectiveness of this material for shielding is exceptionally high (up to 130 dB).[2]

In addition to conventional shielding applications, flexible graphite can serve as a shielding-gasket material because of its resilience. As the resilience of a polymer-matrix composite decreases rapidly with increasing filler content, the attainment of a shielding gasket using a polymer-matrix composite has been a challenge.[15,16]

The high-thermal conductivity, low CTE, high-temperature resistance, and excellent chemical resistance of flexible graphite add to the attraction of this material for use in EMI shielding.

The EMI shielding is achieved by using electrical conductors, such as metals and conductive-filled polymers.[17–19] The EMI shielding gaskets[20–31] are resilient conductors. They are needed to electromagnetically seal an enclosure. The resilient conductors are most commonly elastomers that are filled with a conductive filler or elastomers that are coated with a metallized layer. Metallized elastomers suffer from poor durability due to the tendency of the metal layer to debond from the elastomer. Conductive-filled elastomers do not have this problem, but they require the use of a highly conductive filler, such as silver particles, in order to attain a high shielding effectiveness while maintaining resilience. The highly conductive filler tends to be expensive, making the composite expensive. The use of a less conducting filler results in the need for a large volume fraction of the filler in order to attain a high shielding effectiveness; the consequence is diminished resilience or even loss of resilience. Moreover, these composites suffer from degradation of the shielding effectiveness in the presence of moisture or solvents. In addition, the polymer matrix in the composites limits the temperature resistance, and the thermal expansion mismatch between filler and matrix limits the thermal-cycling resistance. A new class of EMI gasket material is flexible graphite, which is resilient. Although it is not as ductile as silicone, it does not suffer from stress relaxation. Moreover, it is conductive, in addition to being chemically inert and thermally resistant.

This section provides a comparative study of EMI gasket materials, including flexible graphite and conductive-filled elastomers. All materials were tested under identical conditions, using the transfer-impedance method (coaxial-cable method).

Six types of EMI gasket materials were compared. They are (i) flexible graphite, (ii) Ag/Cu particle-filled silicone, (iii) Ag/glass particle-filled silicone, (iv) Ni/carbon particle-filled silicone, (v) carbon black-filled silicone, and (vi) oriented Monel wire-filled silicone.

The shielding effectiveness of the specimens was measured using the coaxial-cable method. The setup, as illustrated in Fig. 1, consists of a shielding-effectiveness tester, connected to a network analyzer. Standard attenuators at 110 dB and 130 dB gave shielding-effectiveness values of 110.2 ± 1.2 dB and 129.0 ± 5.8 dB, respectively. The frequency was scanned from 0.3 MHz to 1.5 GHz. The sample was in the form of an annular ring of an outer diameter of 97 mm and an inner diameter of 32 mm. The resonant frequency of the tester is above 1.5 GHz.

The direct-current (DC), volume-electrical resistivity (in-plane) of each type of material was measured using silver paint for the electrical contacts. For all materials, except (v) and (vi), the four-probe method was used; for materials (v) and (vi), which were relatively high in resistivity, the two-probe method was used. The samples were rectangular bars of length ranging from 14.5–26.3 mm, width ranging from 3.9–5.2 mm, and thickness ranging from 0.79–3.10 mm (Table I). The electrical contacts were around the entire perimeter at planes perpendicular to the length of the bar. In the four-probe method, the outer two contacts were for passing current; the inner two contacts were for voltage measurement. In the two-probe method, each of two contacts were both for passing current and measuring voltage. Four samples were tested for each type of material.

Table I gives the EMI shielding effectiveness in the frequency range from 0.3 MHz to 1.5 GHz. For materials (i), (ii), and (iii), the shielding effectiveness is quite independent of frequency, except for a tail toward low effectiveness at low frequencies. The upper

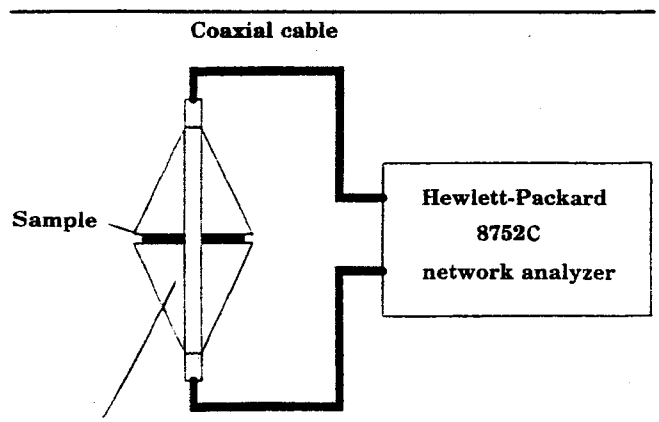

Elgal SET 19A shielding effectiveness tester

Fig. 1. The setup for measuring the EMI shielding effectiveness of various EMI gasket materials.

Table I. The EMI Shielding Effectiveness and DC Electrical Resistivity of Various EMI Gasket Materials

Material	Shielding Effectiveness at 0.3 MHz to 1.5 GHz (dB)	Upper Frequency for Low Shielding Effectiveness (MHz)	Shielding Effectiveness in Frequency Range Outside Tail (dB)	Thickness (mm, ±0.02)	Resistivity (Ωm)
Flexible-graphite A	125.4 ± 5.1	7.8	125.5 ± 5.2	3.10	$(7.5 \pm 0.2) \times 10^{-6}$
Flexible-graphite A	125.4 ± 6.5	37.8	125.6 ± 5.3	1.60	$(7.5 \pm 0.8) \times 10^{-6}$
Flexible-graphite A	122.6 ± 8.9	165.3	125.4 ± 5.4	0.79	$(7.10 \pm 0.03) \times 10^{-6}$
Flexible-graphite B	120.6 ± 7.0	150.3	125.5 ± 5.6	1.14	$(1.6 \pm 0.3) \times 10^{-5}$
Silicone/Ag-Cu	120.4 ± 9.5	150.3	125.5 ± 5.3	3.00	$(7.5 \pm 1.4) \times 10^{-4}$
Silicone/Ag-glass	116.0 ± 12.6	285.3	125.4 ± 5.2	3.00	$(9.8 \pm 0.7) \times 10^{-4}$
Silicone/Ni-C	93.7 ± 14.1	*	*	2.74	$(1.17 \pm 0.13) \times 10^{-3}$
Silicone/carbon black	14.92 ± 0.56	*	*	1.59	$(4.46 \pm 0.15) \times 10^{-3}$
Silicone/oriented wire	0.31 ± 0.13	*	*	1.59	$(1.07 \pm 0.17) \times 10^{3}$

*No tail, as the shielding effectiveness increases gradually with increasing frequency throughout the range from 0.3 MHz to 1.5 GHz.

frequency for the tail is shown in Table I. For materials (iv), (v), and (vi), the shielding effectiveness increases gradually with increasing frequency throughout the range from 0.3 MHz to 1.5 GHz such that there is no tail. The shielding effectiveness is similarly high for materials (i), (ii), and (iii); the values are essentially the same if the tail is excluded. It is lower for material (iv). It is very low for materials (v) and (vi).

Table I also shows the electrical resistivity. The resistivity is particularly low for flexible graphite compared to all other materials investigated. Flexible-graphite A is lower in resistivity and slightly higher in EMI shielding effectiveness than flexible-graphite B. Previous work on shielding was only on the former.[16] Silicone/Ag-glass and silicone/Ag-Cu are quite close in both shielding effectiveness and resistivity. Silicone/Ni-C has higher resistivity than silicone/Ag-Cu or silicone/Ag-glass, and its shielding effectiveness is lower. Silicone/carbon black and silicone/oriented wire are very high in resistivity, and their shielding effectiveness is very low. Silicone/oriented wire has higher resistivity than silicone/carbon black, and its shielding effectiveness is lower. Although the ranking of the shielding effectiveness for the different materials does not exactly follow the ranking of the resistivity, a high shielding effectiveness does correlate with a low resistivity.

The rankings of shielding effectiveness and resistivity do not exactly follow one another. This is due to the skin effect and the consequent importance of the amount of conductor surface area. A high surface area is favorable for shielding. The specific surface area, as determined by nitrogen adsorption and measurement of the pressure of the gas during adsorption, is 15 m^2/g and 10 m^2/g from flexible-graphite A and B, respectively. The higher surface area of the flexible-graphite A contributes to the higher EMI shielding effectiveness of this material.

RESISTIVE HEATING

This section evaluates the effectiveness of flexible graphite as a heating element. The use of flexible graphite as a heating element has been mentioned in patents.[32,33]

Flexible-graphite A, with thicknesses ranging from 0.13–1.17 mm, was evaluated. The specific surface area is 15 m^2/g as determined by nitrogen adsorption. Based on geometric consideration, this specific surface area corresponds to a crystallite layer height of 0.18 μm within a sheet. The ash content of flexible-graphite A is <5.0%; the density is 1.1 g/cm^3; the tensile strength in the plane of the sheet is 5.2 MPa; the compressive strength (10% reduction) perpendicular to the sheet is 3.9 MPa; the thermal conductivity at 1093°C is 43 W/mK in the plane of the sheet and 3 W/mK perpendicular to the sheet; and the CTE (21–1093°C) is -0.4×10^{-6}/°C in the plane of the sheet.

Evaluation of flexible graphite as a heating element was conducted by passing a fixed DC current (ranging from 2–10 A) along the length of the specimen (100 mm × 5 mm in size and thickness ranging from 0.13–1.17 mm) by using electrical contacts (80 mm apart) in the form of silver paint in conjunction with copper wire. The voltage drop (ranging from 0.2–10 V) along the length of the specimen was measured by using two other electrical contacts (60 mm apart); this was also done in the form of silver paint in conjunction with copper wire. During the test, a weight was applied to the top surface of the specimen in order to provide electrical contacts in the form of pressure contacts because the silver paint degraded and lost its adhesive ability as the specimen became hot. The weight was electrically insulated from the specimen by using zirconia fiber cloth. The temperature of the specimen was measured as a function of time during constant current application and in the subsequent period in which the current was off by using a K-type thermocouple located in the middle of the top surface of the specimen. The constant-current period was long enough for the temperature to essentially level off to a maximum.

Figure 2 shows the change in temperature with electrical energy, which is proportional to time because the power (product of voltage and current) is

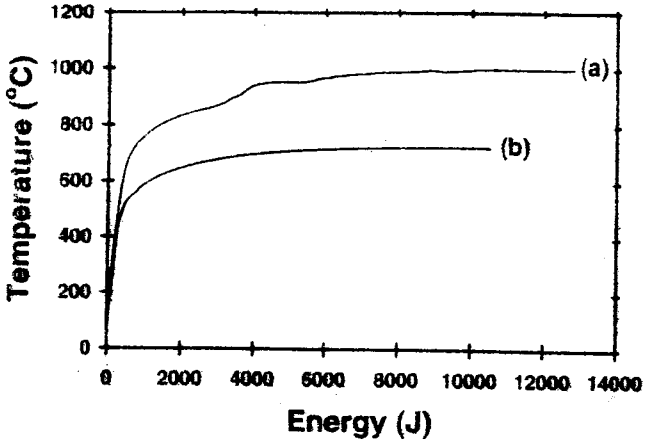

Fig. 2. Temperature vs. electrical energy during heating for a thicknesses of 0.13 mm and power of (a) 94.1 W (9.68 V, 9.72 A) and (b) 52.2 W (6.74 V, 7.75 A).

constant, for two power levels and a thickness of 0.13 mm. For a given power, the temperature increases with energy, as expected, but it levels off gradually. For the same energy, a higher power gives a higher temperature. The data in Fig. 2, together with those for other combinations of power and thickness (Table II), show that the energy needed per °C temperature rise in the initial portion (10–15 sec) of rapid temperature rise is quite independent of thickness and power.

Figure 3 shows the change in temperature with time in the constant-current period and in the subsequent period in which the current is off for two power levels and a thickness of 0.13 mm. The heating is faster than the cooling. The maximum temperature increases with decreasing thickness (Table II) because of the higher resistance associated with a lower thickness. It increases with increasing power (Table II and Fig. 3) as expected. The response time during heating (time to reach

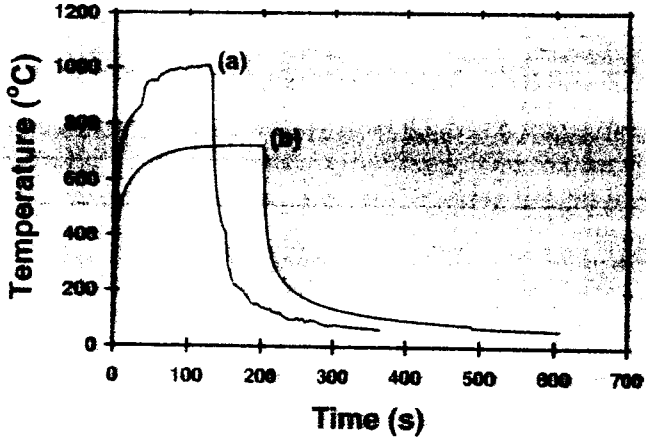

Fig. 3. Temperature vs. time during heating and subsequent cooling for a thickness of 0.13 mm and power of (a) 94.1 W (9.68 V, 9.72 A) and (b) 52.2 W (6.74 V, 7.75 A).

Table II. Performance of Flexible Graphite as a Heating Element

Thickness (mm)	Power (W)	Maximum Temperature (°C)	Time to Reach Half of Maximum Temperature (sec)	Time to Cool to Half of Maximum Temperature (sec)	Energy (J) to Heat by 1°C*	Heat Output (J) at 60 sec
0.13	4.07	108	6	4	1.04	239
0.13	14.6	282	5	6	1.08	861
0.13	31.8	518	5	7	1.14	1880
0.13	52.2	711	4	7	1.15	3091
0.13	94.1	981	4	10	1.25	5588
0.38	1.43	53	6	8	1.43	80
0.38	6.39	149	8	8	1.52	360
0.38	11.74	229	6	8	1.24	666
0.38	21.3	354	5	9	1.38	1210
0.38	31.2	492	6	17	1.86	1785
0.51	0.93	45	6	7	2.10	53
0.51	4.12	89	8	10	1.90	234
0.51	9.56	171	12	8	2.29	545
0.51	16.75	252	9	11	2.16	957
0.51	23.76	327	7	9	2.32	1360
0.76	0.96	33	7	7	2.22	53
0.76	4.07	82	13	8	1.48	224
0.76	8.37	144	5	9	2.25	459
0.76	15.2	219	6	11	1.75	842
0.76	22.6	314	7	10	2.18	1258
1.17	0.48	36	15	11	1.03	24
1.17	1.78	61	9	10	0.87	87
1.17	4.39	109	11	12	1.19	222
1.17	6.88	148	11	15	1.21	352
1.17	10.62	193	9	15	1.55	551

*In the initial portion (10–15 sec) of rapid temperature rise.

half of the maximum temperature) tends to decrease slightly with decreasing thickness; it does not vary monotonically with the power (Table II). The response time during cooling (time to cool to half of the maximum temperature) increases with increasing power for the same thickness, except for the thickness of 0.51 mm, at which no clear trend was observed (Table II).

The highest temperature attained is 981°C, obtained by using the smallest thickness and the highest power. The flexible graphite glows in this case. The temperature increases associated with the fluctuations in the curve for this thickness in Figs. 2a and 3a are attributed to burn-off resulting from oxidation of the graphite.[34,35] The burn-off leads to an increase in resistance and, thus, a rise in temperature. Because of the burn-off, it is not desirable to use flexible graphite as a heating element in air at a power as high as 94 W. At a lower power of 52 W (Figs. 2b and 3b), the fluctuations are absent in the curves because of the relatively minor extent of burn-off. The use of flexible graphite as a heating element in an inert atmosphere will remove the burn-off problem.

The heat output is given by the electrical energy input minus the heat absorbed by the heating element (i.e., flexible graphite). The heat absorbed is given by the product of the specific heat, mass, and temperature change. Assuming that the specific heat is constant at 830 J/kgK (the value for graphite,[36]), the heat output was calculated, as shown in Figs. 4 and 5 for different combinations of thickness and power. After the initial portion (5 sec, Fig. 5), the heat output increases linearly with time because the electrical energy input also increases linearly with time for a given power. For the same thickness and time, the heat output increases with increasing power because the electrical energy input increases with increasing power. For essentially the same power and the same time, the heat output essentially does not vary with the thickness, as shown in Table II for a time of 60 sec.

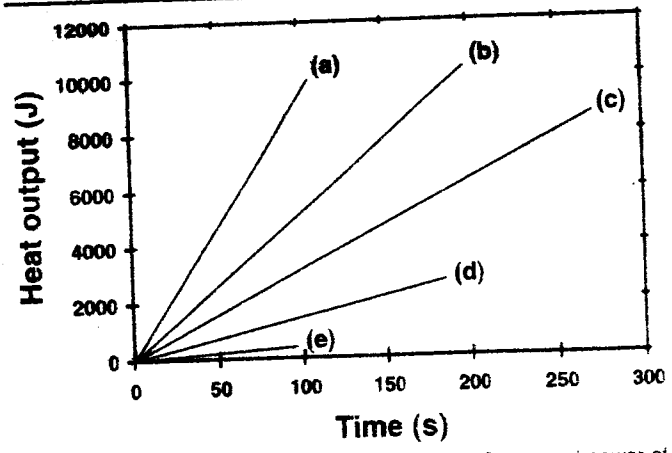

Fig. 4. Heat output vs. time for a thickness of 0.13 mm and power of (a) 94.1 W (9.68 V, 9.72 A), (b) 52.2 W (6.74 V, 7.75 A), (c) 31.6 W (5.29 V, 6.01 A), (d) 14.6 W (3.79 V, 3.86 A), and (e) 4.07 W (2.13 V, 1.91 A).

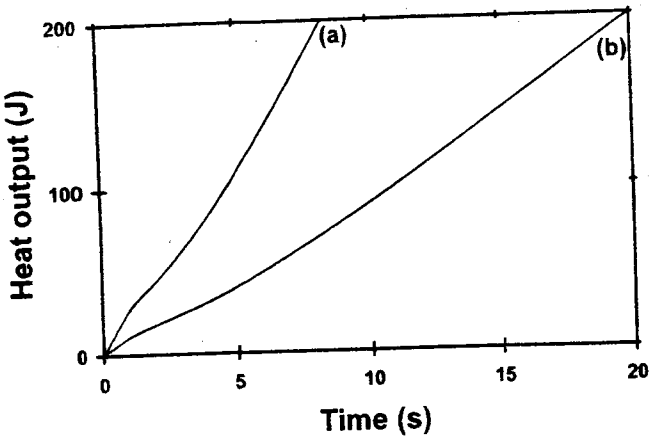

Fig. 5. Heat output vs. time in the initial portion for a thickness of 0.38 mm and power of (a) 31.2 W (3.13 V, 9.97 A) and (b) 11.7 W (2.03 V, 5.78 A).

THERMOELECTRIC-ENERGY CONVERSION

This section addresses the use of flexible graphite as a compliant thermoelectric material. Thermoelectric behavior pertains to the conversion between thermal and electrical energy. In particular, the Seebeck effect is a thermoelectric effect in which a voltage results from a temperature gradient, which causes the movement of charge carriers from the hot point to the cold point. This voltage (Seebeck voltage) is useful for temperature sensing and pertains also to the generation of electrical energy. The negative of the change in Seebeck voltage (hot minus cold) per °C in temperature rise (hot minus cold) is called the thermoelectric power, the thermopower, or the Seebeck coefficient.

The thermal stress between a thermoelectric cell and the wall of a heat exchanger of a thermoelectric-energy conversion system affects the thermal coupling as well as durability. To reduce the thermal stress, compliant pads are used at the interface, although the pad acts as a barrier against thermal conduction.[37,38] If the thermoelectric material is itself compliant, a compliant pad will not be necessary. Compliant polymer-matrix composites containing a thermoelectric filler suffer from their inability to withstand high temperatures, as encountered in thermoelectric-power conversion systems with a high thermal-energy density. Flexible graphite is compliant and resistant to high temperatures, in addition to being a thermoelectric material.[39]

Metals are, in general, more compliant than semiconductors, but their Seebeck effect is relatively weak, and they tend to suffer from corrosion. Polymers can be more compliant than metals, but they are usually electrically insulating and do not exhibit the Seebeck effect. Flexible graphite is quite unusual in its combination of compliance and strong thermoelectric behavior.

The Seebeck effect tends to be weaker in metals than in semiconductors, but metals are more conductive electrically than semiconductors. This means that attaining a large Seebeck effect is not

simply a matter of increasing the carrier concentration or mobility. A low thermal conductivity helps, as it enables a steep temperature gradient to occur, thereby decreasing the flow distance of the carrier.

Flexible graphite is much more conductive thermally in the in-plane direction than in the out-of-plane direction. The high in-plane thermal conductivity, together with the resilience in the out-of-plane direction, helps the attaining of a good thermal contact between flexible graphite and a hot/cold surface. On the other hand, the low out-of-plane thermal conductivity is favorable for the Seebeck effect in the out-of-plane direction.

The Seebeck effect in the through-thickness direction of flexible graphite can be used for the generation of electrical energy, as a Seebeck voltage is generated between the two opposite in-plane surfaces of a flexible-graphite sheet when the sheet is placed on a hot object (such as a human body) or a cold object (such as the window of an aircraft). The flexibility of the sheet facilitates the placement on a surface that is not flat. A related application is the sensing of the temperature of the hot or cold object.

Flexible-graphite A was evaluated. The thermoelectric behavior in the through-thickness direction was investigated using the following method. A specimen of size 25.9 mm × 24.9 mm × 1.17 mm was placed on an insulator-lined hot plate. Thus, a temperature gradient was generated in the through-thickness direction. The hot plate was controlled by a temperature controller, which provided a heating rate of 0.174°C/min. and a cooling rate of 0.167°C/min. The voltage difference between the top and bottom surfaces was measured by using electrical contacts in the form of silver paint in conjunction with copper wire. The temperatures of the top and bottom surfaces were simultaneously measured by using two T-type thermocouples. The temperature of the hot side ranged from 21–111°C, and the temperature of the cold side ranged from 21–49°C. The temperature difference was up to 62°C. The cold side was cooled by using air, which was blown through a steel pipe in the direction perpendicular to the specimen surface. The extent of cooling depended on the air flow conditions.

Figure 6 shows the measured voltage difference vs. the temperature difference during heating. The hundreds of data points essentially fall on a straight line through the origin. The slope of the line gives a thermoelectric power (relative to that of copper) of −0.65 μV/°C. This Seebeck coefficient minus the absolute thermoelectric power of copper (+1.94 μV/°C at 300 K)[40] is the absolute thermoelectric power of the specimen. The absolute thermoelectric power is thus −2.6 μV/°C. The behavior was quantitatively similar during cooling; the slope of the curve was the same.

The thermoelectric power has been previously reported for flexible graphite,[39] kish graphite,[41,42] highly oriented pyrolytic graphite,[41,43] carbon fibers,[44,45] and graphite intercalation compounds.[46,47] For carbons that have not been intercalated, both positive and negative values of the absolute thermoelectric power at room temperature have been reported. The value depends on the crystallinity, defects, phonons, and impurities, in addition to the carrier type and concentration.

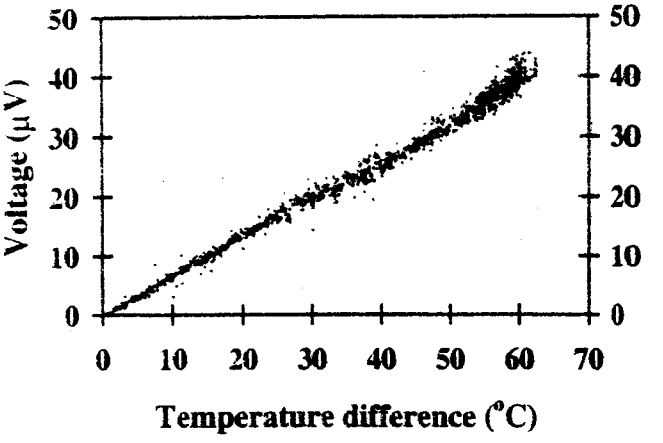

Fig. 6. Measured voltage difference vs. temperature difference between the top and bottom surfaces of a flexible-graphite sheet during heating.

The value of −2.6 μV/°C reported here for flexible graphite in the through-thickness direction near room temperature in the absence of a magnetic field is comparable to but more negative than that previously reported for a flexible graphite of density 0.82 g/cm^3.[39] The difference in density is a factor that contributes to the difference in thermoelectric power.

Relative to other carbons, the value reported here is attributed to the combination of crystallinity, c-axis electrical connectivity, and in-plane preferred orientation of the carbon layers. In particular, the unique microstructure of flexible graphite compared to other carbons is probably a factor.

HEAT DISSIPATION

This section addresses the use of flexible graphite as a thermal-interface material. Thermal-interface materials[48] are needed to improve thermal contacts. By placing a thermal-interface material at the interface between two components across which heat must flow, the thermal contact between the two components is improved. A primary market for thermal-interface materials is in the electronic industry, as heat dissipation is critical to the performance, reliability, and further miniaturization of microelectronics. For example, a thermal-interface material is used to improve the thermal contact between a heat sink and a printed circuit board or between a heat sink and a chip carrier.

A thermal-interface material can be a thermal fluid, a thermal grease (paste), a resilient thermal conductor, or solder that is applied in the molten state. A thermal fluid, thermal grease, or molten solder is spread on the mating surfaces. A resilient thermal conductor is sandwiched by the mating surfaces and held in place by pressure. Thermal fluids

are most commonly mineral oil. Thermal greases (pastes) are the most common conducting particle-filled (usually metal or metal oxide) silicone. Resilient thermal conductors are the most common conducting particle-filled elastomers. Out of these four types of thermal-interface materials, thermal greases (based on polymers, particularly silicone) and solder are by far most commonly used. Resilient thermal conductors are not as well developed as thermal fluids or greases.

As the materials to be interfaced are good thermal conductors (such as copper), the effectiveness of a thermal-interface material is enhanced by high thermal conductivity and low thickness of the interface material and low thermal-contact resistance between the interface material and each mating surface. As the mating surfaces are not perfectly smooth, the interface material must be able to flow or deform in order to conform to the topography of the mating surfaces. If the interface material is a fluid, grease, or paste, it should have a high fluidity (workability) so as to conform and have a small thickness after mating. On the other hand, the thermal conductivity of the grease or paste increases with increasing filler content, and this is accompanied by decrease in the workability. Without a filler, as in the case of an oil, the thermal conductivity is poor. A thermal-interface material in the form of a resilient thermal-conductor sheet (e.g., a felt consisting of conducting fibers clung together without a binder, a resilient polymer-matrix composite containing a thermally conducting filler, or flexible graphite) usually cannot be as thin or conformable as one in the form of a fluid, grease, or paste, so its effectiveness requires a very high thermal conductivity within it.

Solder is commonly used as a thermal-interface material for enhancing the thermal contact between two surfaces. This is because solder can melt at rather low temperatures, and the molten solder can flow and spread itself thinly on the adjoining surfaces, thus resulting in high thermal-contact conductance at the interface between solder and each of the adjoining surfaces. Furthermore, solder in the metallic solid state is a good thermal conductor. In spite of the high thermal conductivity of solder, the thickness of the solder greatly affects the effectiveness of the solder as a thermal-interface material; a small thickness is desirable.[49] Moreover, the tendency for solder to react with copper to form intermetallic compounds[50] reduces the thermal-contact conductance of the solder/copper interface.

Thermal pastes are predominantly based on polymers, particularly silicone,[51–54] although thermal pastes based on sodium silicate have been reported to be superior in providing high thermal-contact conductance.[55] The superiority of sodium-silicate-based pastes over silicone-based pastes is primarily due to the low viscosity of sodium silicate, compared to silicone, and the importance of high fluidity in the paste so that the paste can conform to the topography of the surfaces that it interfaces.

A particularly attractive thermal paste is based on polyethylene glycol (PEG, a polymer) of a low molecular weight (400 amu).[56] These pastes are superior to silicone-based pastes and are as good as sodium-silicate-based pastes due to the low viscosity of PEG and the contribution of lithium ions (a dopant) in the paste to thermal conduction. Compared to the sodium-silicate-based pastes, the PEG-based pastes are advantageous in their long-term compliance, which is in contrast to the long-term rigidity of sodium silicate. Compliance is attractive for decreasing the thermal stress, which can cause thermal fatigue.

This section provides an evaluation of flexible graphite as a thermal-interface material. The evaluation is motivated by the resilience, thermal conductivity, low thermal expansion, thermal stability, and chemical inertness of flexible graphite. Because the method of evaluation used in this work is the same as that of previous work[49,55,56] on competing thermal-interface materials, this section provides a comparative study.

Flexible-graphite sheets of thickness ranging from 0.13–0.38 mm were evaluated. Four grades of flexible graphite were used, namely GTA, GTB (same as flexible-graphite A mentioned previously), GTC, and Toyo, which have carbon contents 99%, 95%, 80%, and 95%, respectively. This work emphasizes GTB.

Flexible-graphite sheets of various combinations of grade (carbon content), density, and thickness were sandwiched between the flat surfaces of two copper disks (both surfaces of each disk having been mechanically polished by using 0.05-μm alumina particles), each having a diameter of 12.6 mm with one having a thickness of 1.16 mm and the other a thickness of 1.10 mm. The thermal-contact conductance between two copper disks with and without a thermal-interface material was measured using the transient-laser flash method.[55,57,58] The pressure on the sandwich was controlled at 2.2 MPa, 6.7 MPa, or 11.1 MPa. This is because the pressure affects the thermal-contact conductance even for a material that is not resilient.[55]

The finite element program *ABAQUS* (Version 5.8, 1988, Hibbitt, Karlsson and Sorrensen, Inc., Pawtucket, RI) was used to calculate the thermal-contact conductance through temperature vs. time curves, which were experimentally obtained. The calculation[55] assumed no thickness and no heat capacity for the interface between the two copper disks. In addition, it assumed no heat transfer between specimen and environment except for the absorption of laser energy by the specimen. Moreover, it assumed that the laser energy was uniformly absorbed on the surface of the specimen, that the heat flow was one-dimensional, and that the thermal-contact conductance between the two copper disks was uniform. The validity of these assumptions is supported by the calibration result and error analysis given subsequently.

A Nd-glass laser with a pulse duration of 0.4 ms, a wavelength of 1.06 μm, and a pulse energy up to 15 J was used for impulse heating. The temperature rise of the specimen was between 1°C and 2°C. The upper surface of disk 1, on which the laser beam would directly hit, had been electroplated by black nickel in order to increase the extent of laser-energy absorption relative to the extent of reflection (Fig. 7). An E-type thermocouple (1) was attached to the back surface of disk 2 for monitoring the temperature rise. Another thermocouple (2) of the same type was put ~30 cm above the specimen holder to detect the initial time when the laser beam came out. A data-acquisition board with a data-acquisition rate up to 20,000 data points per second at 16 bytes resolution was used to monitor the response of both thermocouples simultaneously. An acrylic (Plexiglas, ATOFINA Chemicals, Inc., Atoglas Div., Philadelphia, PA) holder (Fig. 7) was used to facilitate pressure application. A load cell was used for pressure measurement. Calibration using a standard graphite specimen was performed in order to ensure measurement accuracy. The data-acquisition rate used for each test was adjusted so that there were at least 100 temperature-data points during the temperature rise.

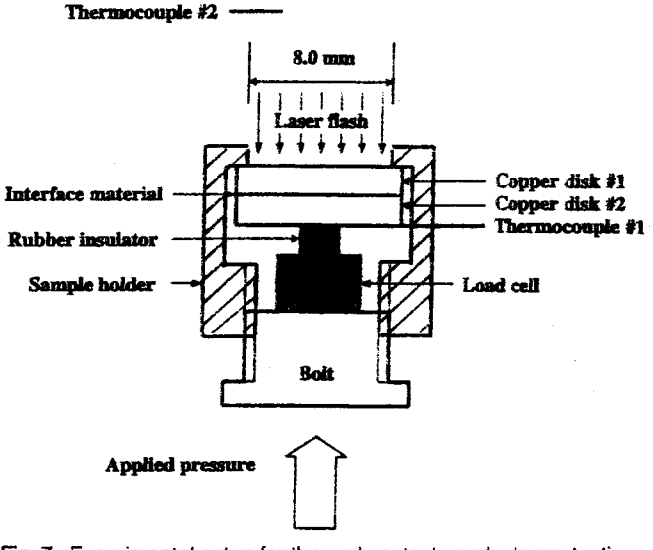

Fig. 7. Experimental setup for thermal contact-conductance testing.

The experimental error in transient thermal-contact conductance measurement consists of random error due to experimental data scatter and systematic error because of the lag of the thermocouple response and partly because of the method used to calculate the conductance from the temperature data. The higher the thermal-contact conductance, the greater the error. The thermal diffusivity of a standard NBS 8426 graphite disk (thickness = 2.62 mm), which had a similar transient temperature-rise time as the copper sandwich with the highest thermal-contact conductance, was measured prior to testing each specimen in order to determine the systematic error. The measured thermal diffusivity of the graphite was about 7% less than the reference value, which corresponds to a time lag of about 0.0006 sec. Moreover, a single copper disk (thickness = 2.66 mm) was also tested, and a time lag of about 0.0008 sec was found upon comparison of the measured thermal diffusivity with the reference value. From multiple measurements of both copper and graphite, the time lag of the thermocouple was found to be about 0.0007 sec, which was used to correct for the measured rise time for each specimen. The conductance reported for each sample was based on the corrected rise time. The random error shown by the ± value was determined by the measurement of 2–3 (usually 3) specimens.

Table III gives the thermal-contact conductance attained by using flexible graphite of grade GTB as the thermal-interface material.

The conductance increases with pressure, as expected. The pressure dependence is particularly significant for the lowest thickness of 0.13 mm because of the importance of conformability, which increases with increasing thickness.

A decrease in thickness enhances the conductance for each combination of pressure and density, except at the pressure of 2.2 MPa and the thickness of 0.13 mm. This trend is expected because a thicker interface material gives more thermal resistance within itself.

Table III. Thermal-Contact Conductance Attained Using Flexible Graphite of Grade GTB as the Thermal-Interface Material

Thickness* (mm)	Density (g/cm^3)	Contact Conductance (10^4 W/m^{2}K) 2.2 MPa	6.7 MPa	11.1 MPa
0.13	1.1	2.06 ± 0.06	3.60 ± 0.09	4.59 ± 0.09
0.13	1.4	0.94 ± 0.01	1.80 ± 0.06	2.95 ± 0.17
0.25	0.8	0.86 ± 0.01	1.03 ± 0.01	1.05 ± 0.03
0.25	1.1	2.24 ± 0.13	2.39 ± 0.09	2.49 ± 0.20
0.25	1.4	1.54 ± 0.01	2.15 ± 0.02	2.23 ± 0.01
0.38	0.8	—	0.82 ± 0.03	0.87 ± 0.01
0.38	1.1	1.47 ± 0.01	1.68 ± 0.02	1.95 ± 0.01
0.38	1.4	1.12 ± 0.01	1.40 ± 0.08	2.09 ± 0.01
—	—	0.75 ± 0.01**	1.07 ± 0.02**	1.59 ± 0.02**

*Thickness of flexible graphite in the absence of pressure.
**Without a thermal-interface material.

Table IV. Thermal-Contact Conductance Attained Using Flexible Graphite of 1.1 g/cm³ Density and 0.38 mm Thickness (Value without Pressure) as the Thermal-Interface Material

Grade	Carbon Content (Wt.%)	Contact Conductance (10^4 W/m²K) 2.2 MPa	6.7 MPa	11.1 MPa
GTA	99	1.47 ± 0.21	1.87 ± 0.03	2.06 ± 0.01
GTB	95	1.47 ± 0.01	1.68 ± 0.02	1.95 ± 0.01
GTC	80	1.53 ± 0.01	1.67 ± 0.19	2.20 ± 0.02
Toyo	95	0.88 ± 0.01	0.89 ± 0.01	0.99 ± 0.02

An increase in density enhances the conductance when the thickness is large (0.38 mm) but decreases the conductance when the thickness is low (0.13 mm). At the intermediate thickness of 0.25 mm, the conductance is highest at the intermediate density (1.1 g/cm³). The trend of increasing conductance with increasing density is due to the increase in thermal conductivity of the flexible graphite with increasing density. For a large thickness, the thermal resistance within the flexible graphite is particularly important. The trend of decreasing conductance with increasing density is due to the decrease in conformability with increasing density. For a small thickness, the conformability is particularly important.

Among the various combinations of thickness and density, the combination that gives the highest conductance is that for the lowest thickness (0.13 mm) and the lowest density (1.1 g/cm³) available for a thickness of 0.13 mm. The highest conductance, as attained at a pressure of 11.1 MPa, is 4.6×10^4 W/m²K. This value is low compared to the value of 21×10^4 W/m²K, attained by using solder at zero contact pressure,[56] and the value of 19×10^4 W/mK, attained by using a polyethylene-glycol-based paste at a contact pressure of 0.46 MPa.[56] The requirement of a high contact pressure is a disadvantage of flexible graphite.

Included in Table III are the conductance values for the case of no interface material. Flexible graphite as an interface material gives even lower conductance than the case of no interface material if the thickness is high (0.25 mm or above), and the density is low (0.8 g/cm³).

Table IV shows that the ash content (the content other than carbon) of flexible graphite has little effect on the conductance.

CONCLUSIONS

Electronic applications of flexible graphite are feasible. Flexible graphite is comparable to or better than conductive-filled silicone materials, including silicone filled with Ag-Cu particles, for EMI gasketing. The shielding effectiveness reaches 125 dB at 0.3 MHz to 1.5 GHz and is a consequence of the low electrical resistivity and high specific surface area.

Flexible graphite is an effective heating element. It provides temperatures up to 980°C (though burnoff occurs in air at 980°C), response half-time down to 4 sec, and heat output at 60 sec up to 5600 J. The electrical energy for heating by 1°C is 1–2 J in the initial portion of rapid temperature rise. The temperature and heat output increase with decreasing thickness and with increasing power.

The through-thickness absolute thermoelectric power of flexible graphite is −2.6 μV/°C near room temperature. The effect, together with the flexibility of the material, makes the thermoelectric phenomenon potentially useful for temperature sensing and thermoelectric-power generation.

Flexible graphite is effective as a thermal-interface material if the thickness is low (0.13 mm), the density is low (1.1 g/cm³), and the contact pressure is high (11.1 MPa). The effectiveness of flexible graphite as a thermal-interface material is much lower than those of solder and thermal pastes, and flexible graphite requires much higher contact pressure than these other interface materials. However, flexible graphite is attractive in its thermal stability.

REFERENCES

1. D.D.L. Chung, *J. Mater. Eng. Perform.* 9, 161 (2000).
2. X. Luo and D.D.L. Chung, *Carbon* 34, 1293 (1996).
3. M. Toyoda, J. Aizawa, and M. Inagaki, *Desalination* 115, 199 (1998).
4. N.N. Avgul', N.V. Kovaleva, I.L. Mar'yasin, and G.A. Mishina, *Coll. J. USSR* (English translation of *Koll. Z.*) 44, 274 (1982).
5. L.C. Olsen, S.E. Seeman, and H.W. Scott, *Carbon* 8, 85 (1970).
6. D.D.L. Chung and L.W. Wong, *Synth. Met.* 12, 533 (1985).
7. M. Rommler, *Am. Soc. Mech. Eng., Pressure Vessels Piping Div.* 382, 37 (1999).
8. M. Derenne, L. Marchand, and J.R. Payne, *Materials Manufacturing Proc. 1996, 8th Int. Conf. Pressure Vessel Technology*, ICPVT, vol. 1 (New York: ASME, 1996), p. 125.
9. W.F. Jones and B.B. Seth, *J. Test. Eval.* 21, 94 (1993).
10. A. Bazergui and J.R. Winter, *Am. Soc. Mech. Eng., Pressure Vessels Piping Div.* 156, 33 (1989).
11. M. Derenne, L. Marchand, and J.R. Payne, *Welding Res. Council Bull.* 419, 1 (1997).
12. X. Luo and D.D.L. Chung, *Carbon* 38, 1510 (2000).
13. C.A. Frysz and D.D.L. Chung, *Carbon* 35, 858 (1997).
14. X. Luo and D.D.L. Chung, *J. Intelligent Mater. Sys. Struct.* 8, 389 (1997).
15. R. Bates, S. Spence, J. Rowan, and J. Hanrahan, *8th Int. Conf. Electromagnetic Compatibility* (London: Institution of Electrical Engineers, 1992), p. 246.
16. J.A. Catrysse, *8th Int. Conf. Electromagnetic Compatibility* (London: Institution of Electrical Engineers, 1992), p. 251.
17. J. Wang, V.V. Varadan, and V.K. Varadan, *SAMPE J.* 32, 18 (1996).

18. S. Maudgal and S. Sankaran. *Proc. Nat. Conf.*, ed. O.P. Bahl (Delhi, India: Shipra Publ., 1997), p. 12.
19. J.T. Hoback and J.J. Reilly. *J. Elastomers Plast.* 20, 54 (1988).
20. P. O'Shea, *Eval. Eng.* 34, 84 (1995).
21. R.A. Rothenberg, D.C., Inman, and Y. Itani, IEEE *Int. Symp. Electromagnetic Compatibility* (Piscataway, NJ: IEEE, 1994), p. 818.
22. P. O'Shea, *Eval. Eng.* 35, 56 (1996).
23. J.W.M. Child, *Electron. Prod.* Oct., 41, (1986).
24. A.K. Subramanian, D.C. Pande, and K. Boaz, *Proc. 1995 Int. Conf. Electromagnetic Interference Compatibility* (Madras, India: Society of EMC Engineers, 1995), p. 139.
25. W. Hoge, *Eval. Eng.* 34, 84 (1995).
26. J.F. Walther, *IEEE 1989 Int. Symp. Electromagnetic Compatibility: Symp. Record* (New York: IEEE, 1989), p. 40.
27. H.W. Denny and K.R. Shouse, *IEEE 1990 Int. Symp. Electromagnetic Compatibility: Symp. Record* (New York: IEEE, 1990), p. 20.
28. A.N. Faught, *IEEE Int. Symp. Electromagnetic Compatibility* (New York: IEEE, 1982), p. 38.
29. G. Kunkel, *IEEE Int. Symp. Electromagnetic Compatibility* (New York: IEEE, 1980), p. 211.
30. R.E. Rapp, L.D. Dillon, and H. Godfrin, *Cryogenics* 25, 152 (1985).
31. Y. Hishiyama, Y. Kaburagi, and K. Sugihara. *Mol. Cryst. Liq. Cryst.* 340, 337 (2000).
32. K.H. Hsu, J.R. Payne, and M. Derenne, *Proc. 1993 Pressure Vessels Piping Conf. on Power Plant Equipment Design: Bolted Joints, Pumps, Valves, Pipe Duct Supports* (New York, NY: American Society of Mechanical Engineers, 1993), vol. 255, p. 65.
33. M. Asahina, T. Nishida, and Y. Yamanaka, *Proc. 1996 ASME Pressure Vessels Piping Conf. Computer Technology–Applied Methodology* (New York, NY: American Society of Mechanical Engineers, 1996), vol. 326, p. 47.
34. W.D. Callister, Jr., *Materials Science and Engineering*, 5th ed. (New York: John Wiley and Sons, Inc., 2000), p. 811.
35. M. Kambe, *Mater. Sci. Forum* 308–311, 653 (1999).
36. M. Arai, M. Kambe, T. Ogata, and Y. Takahashi, *Nippon Kikai Gakkai Ronbunshu, a Hen* 62, 488 (1996).
37. C. Uher, *Phys. Rev. B* 25, 4167 (1982).
38. R.B. Roberts, *CODATA Bull.* 59, 47 (1985).
39. Y. Hishiyama and A. Ono, *Carbon* 23, 445 (1985).
40. Y. Kaburagi and Y. Hishiyama, *Carbon* 36, 1671 (1998).
41. A. Ono and Y. Hishiyama, *Philos. Mag. B* 59, 271 (1989).
42. J.P. Heremans, *Extended Abstracts and Program—17th Biennial Conf. on Carbon* (University Park, PA: American Carbon Society, 1985), pp. 231–232.
43. J. Tsukamoto, A. Takahashi, T. Tani, and T. Ishiguro, *Carbon* 27, 919 (1989).
44. C. Uher and D.T. Morelli, *Synth. Met.* 12, 91 (1985); *Graphite Intercalation Compounds, Proc. Int. Symp.* (1985), pp. 91–96.
45. K. Kobayashi, K. Sugihara, and H. Oshima, *J. Phys. Chem. Solids* 57, 931 (1996).
46. D.D.L. Chung, *J. Mater. Eng. Perform.* 10, 56 (2001).
47. X. Luo and D.D.L. Chung, *Int. J. Microcir. Electron. Packag.* 24, 141 (2001).
48. D. Grivas, D. Frear, L. Quan, and J.W. Morris, Jr., *J. Electron. Mater.* 15, 355 (1986).
49. S.W. Wilson, A.W. Norris, E.R. Scott, and M.R. Costello, *Proc. Technical Program, Nat. Electronic Packaging Production Conf.* (Norwalk, CT: Reed Exhibition Companies, 1996), vol. 2, p. 788.
50. A.L. Peterson, *Proc. 40th Electronic Components Technology Conf.* (Piscataway, NJ: IEEE, 1990), vol. 1, p. 613.
51. X. Lu, G. Xu, P.G. Hofstra, and R.C. Bajcar, *J. Polym. Sci., Part B: Polym. Phys.* 36, 2259 (1998).
52. T. Sasaski, K. Hisano, T. Sakamoto, S. Monma, Y. Fijimori, H. Iwasaki, and M. Ishizuka, *Japan IEMT Symp. Proc., IEEE/CPMT Int. Electronic Manufacturing Technology (IEMT) Symp.* (Piscataway, NJ: IEEE, 1995), p. 236.
53. Y. Xu, X. Luo, and D.D.L. Chung, *J. Electron. Packaging* 122, 128 (2000).
54. Y. Xu, X. Luo, and D.D.L. Chung, *J. Electron. Packaging*, in press.
55. W.J. Parker, R.J. Jenkins, C.P. Butler, and G.L. Abbott, *J. Appl. Phys.* 32, 1679 (1961).
56. K. Inoue and E. Ohmura, *Yosetsu Gakkai Ronbunshu/Q. J. Jpn. Welding Soc.* 6, 130 (1988).